TITLE:

A New Design of Mode-Matched (100) Silicon Ring Gyroscope with Chamfered Rectangle Springs Immune to Fabrication Error

AUTHOR(S):

Okayama, Shuya; Banerjee, Amit; Hirotani, Jun; Tsuchiya, Toshiyuki

CITATION:

Okayama, Shuya ...[et al]. A New Design of Mode-Matched (100) Silicon Ring Gyroscope with Chamfered Rectangle Springs Immune to Fabrication Error. 2023 IEEE International Symposium on Inertial Sensors and Systems (INERTIAL) 2023

ISSUE DATE:

2023

URL:

http://hdl.handle.net/2433/284809

RIGHT:

© 2023 IEEE. Personal use of this material is permitted. Permission from IEEE must be obtained for all other uses, in any current or future media, including reprinting/republishing this material for advertising or promotional purposes, creating new collective works, for resale or redistribution to servers or lists, or reuse of any copyrighted component of this work in other works.; This is not the published version. Please cite only the published version. この論文は出版社版でありません。引用の際には出版社版をご確認ご利用ください。

京都大学学術情報リポジトリ
KURENAI 紅
Kyoto University Research Information Repository

京都大学 KYOTO UNIVERSITY
A Self-archived copy in
Kyoto University Research Information Repository
https://repository.kulib.kyoto-u.ac.jp
京都大学学術情報リポジトリ KURENAI 紅 Kyoto University Research Information Repository

A New Design of Mode-Matched (100) Silicon Ring Gyroscope with Chamfered Rectangle Springs Immune to Fabrication Error

Shuya Okayama, Amit Banerjee, Jun Hirotani and Toshiyuki Tsuchiya
Department of Micro Engineering, Kyoto University
Kyoto 615-8540, Japan
s_okayama@nms.me.kyoto-u.ac.jp, {banerjee.amit.3v, hirotani.jun.7v}@kyoto-u.ac.jp, tutti@me.kyoto-u.ac.jp

***Abstract*—In this report, we proposed a new design of mode-matched (100) single crystal silicon (SCS) ring gyroscope immune to fabrication errors. The robustness against dimensional and orientation errors was confirmed by finite element analysis simulations and frequency response measurements. The designed ring resonator has a ring of uniform width suspended by eight identical suspension structures and it has eight-fold symmetry. The in-plane elastic asymmetry of the ring is compensated by the carefully designed suspension structures with four rectangular beams with two chamfered corners in each. As a simulation result, we found that the optimum chamfering size for the ring width of 5.1 μm and the diameter of 2 mm and the ring resonator is almost insensitive to fabrication errors. The resonators were fabricated using silicon-on-insulator wafers and the as-fabricated device shows small mismatch about 0.5 – 1.5%, which is caused by the nonuniform fabrication errors. After electrostatic tuning, gyro output was successfully measured.**

Keywords—vibrating gyroscope, (100) silicon, mode match, fabrication error

I. Introduction

For small-size, low-cost and high-performance gyroscopes, wine-glass mode vibratory gyroscopes using the microelectromechanical system (MEMS) technology are attracting attentions. Their performance depends on the in-plane isotropy of the resonator stiffness, so axisymmetric gyroscopes, for example, ring [1], disk [2][3], and cylinder [4], have been employed. Especially, the whole angle mode which is one of the control schemes for operating gyroscopes [5], which has low temperature sensitivity, requires zero difference between resonant frequencies of two wineglass modes, called as perfect mode-matching. In Ref. [1][2], mode-matched axis-symmetric gyroscopes have been proposed using (100) SCS whose fabrication cost is low compared to isotropic materials such as (111) SCS [4] and polysilicon [3]. To compensate anisotropic in-plane stiffness of (100) SCS, the design whose ring width varied with orientation has been proposed and demonstrated [1]. However, the experimental results showed their poor robustness against fabrication errors in dimensions and crystal orientations. In this study, we proposed a new design which utilizes symmetric structures immune to fabrication errors in dimensions and crystal orientations. In this paper, we report the proposed suspension beams structures and a resonator design to realize mode-matching and fabrication error robustness. Then the experimental verification and operation as a vibrating gyroscope are reported.

II. Ring Resonator Design

A. Suspention with chamfered rectangler beams

We designed the ring resonator which consists of a uniform-width ring and eight identical suspension structures, as shown in Fig. 1. The radius and thickness of the resonator are 1000 μm and 22 μm, respectively, and the anchor radius is 200 μm. The suspension is a radial beam inserting four chamfered rectangular beams with the same interval. The radial side lengths of the rectangular beams $L_1 + L_2$ are 110 μm. In the case of the suspensions oriented for 0°, shown in the inset of Fig. 1, the beams along the radial and tangential directions have the maximum Young's modulus of {110} direction, and beams of the chamfered parts have the minimum Young's modulus of {100} direction. Therefore, the stiffness of the suspension structure against the radial force increases when the chamfering parts are longer. On the other hand, when the suspensions oriented for 45° its stiffness decreases. Using these properties, the anisotropy of the ring stiffness is compensated by controlling the chamfered part ratio, L_1/L_2 . Finite element analysis (CoventorWare,

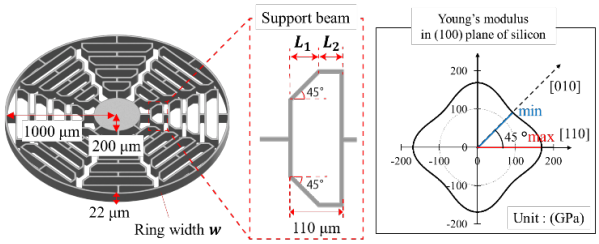

Fig. 1. (left) Ring resonator design and (right) in-plane Young's modulus of (100) silicon

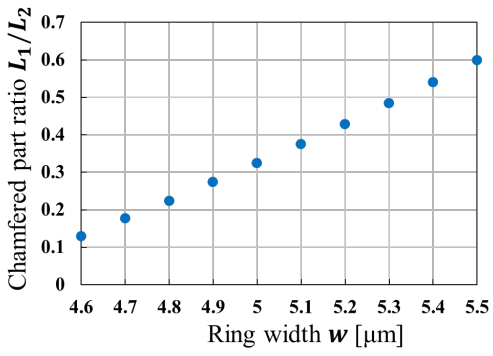

Fig. 2. Chamfered part ratio L_1/L_2 of mode-matched designs as a function of ring width w.

京都大学 KYOTO UNIVERSITY
A Self-archived copy in
Kyoto University Research Information Repository
https://repository.kulib.kyoto-u.ac.jp
京都大学学術情報リポジトリ KURENAI 紅 Kyoto University Research Information Repository

Coventor) was conducted to get the relationship between the chamfered part ratio L_1/L_2 and the ring widths. The width W_s of the support beam, including the chamfered rectangular beams, width is set to 5 μm and the ring width W_r is varied. Fig.2 shows the simulated ratio L_1/L_2 as a function of the ring width W_r where the mode match is obtained. The wider the ring is, the chamfered part ratio increases.

B. Robustness simulation against fabrication errors

We examined the robustness in mode-matching of the proposed ring design against dimensional and crystal orientation alignment errors. The dimensional error is occurred on mask fabrication, photolithography, and etching prosses steps. In the FEM analysis, an uniform dimensional error of -0.8 μm which was observed in Ref [1], was assumed. The mode mismatch with the dimensional error for the design sets with the ratio and widths shown in Fig. 2 was simulated. The obtained mode mismatch against the width W_s is shown in Fig. 3. At the ring width W_r of 5.1 μm and the L_1/L_2 of 0.375, there is almost no effect of the dimensional errors on the mode-mismatch. Fig. 4a shows the mismatch as a function

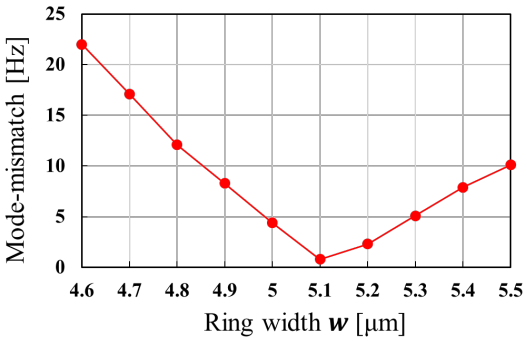

Fig. 3. Mode mismatch of designs shown in Fig.2 by adding fabrication errors of -0.8 μm.

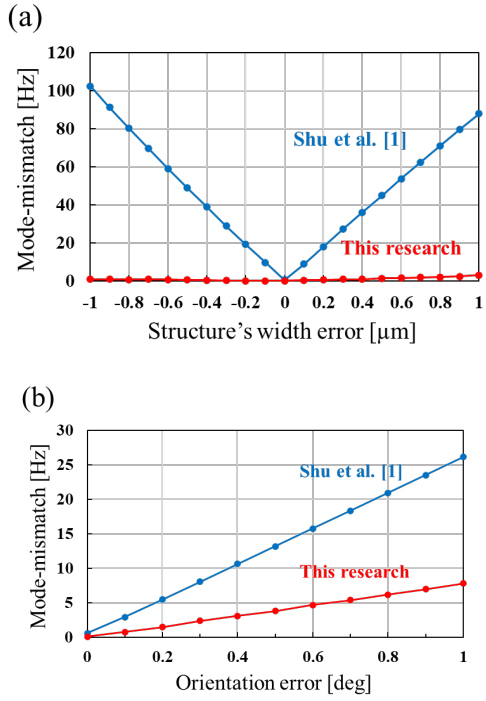

Fig. 4. Mode mismatch as a function of (a) structure's width error and (b) orientation error

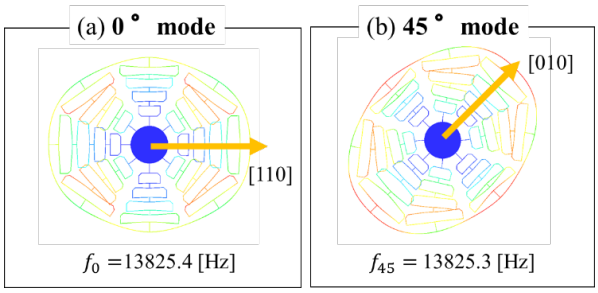

Fig. 5. Wineglass mode shapes of optimized resonator having smallest sensitivity to fabrication errors. The ring width is 5.1 μm and the chamfered part ratio L_1/L_2 is 0.375. (a) 0° mode and (b) 45° mode

of the dimensional errors of this design and the previous work [1]. The effect of dimensional error is significantly reduced.

The crystal orientation alignment error occurs by the wafer misorientation and photolithography process. As we described above, The designed beams in the suspensions consist of only {100} and {110} oriented beams. The design has also small effect of angular misorientations, since the stiffness of these two direction is local maximum. Fig. 4b shows the mode mismatch as a function of the orientation angle error. The sensitivities of the mode-mismatch are 30 % compared to our previous work [1]. These results show that the proposed resonator has the potential for a high-performance whole angle mode gyroscope.

Therefore we set the ring width W_r as 5 μm. The mode shapes of the two wine glass modes were simulated. The resonant frequencies are 13825.4 Hz (0°) and 13825.3 Hz (45°), as the mode shapes are shown in Fig. 5.

III. Experiments

A. Device fabrication

The designed resonator was fabricated on silicon-on-insulator (SOI) wafers of 22-μm-thick device layer and 2-μm-thick buried oxide layer. After deposition and pattering of Au/Cr films for electrodes, the device layer was patterned using UV contact lithography and deep reactive ion etching (RIE). The sacrificial layer was etched by vapor hydrofluoric acid (HF) to release the resonator structure. Then the wafer was diced into chips using a laser dicer. The chips were mounted on ceramic packages.

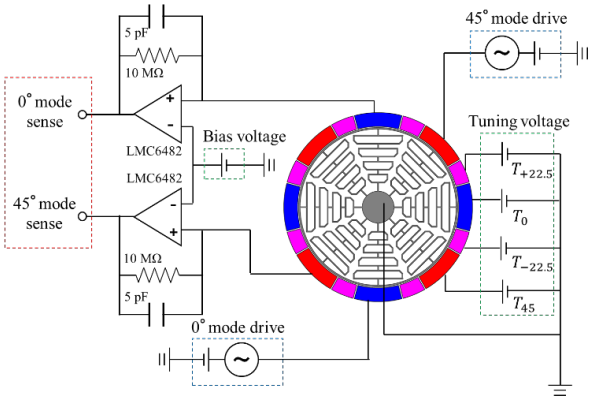

Fig. 6. Electrical connection for driving, sensing and tuining control.

京都大学 KYOTO UNIVERSITY
A Self-archived copy in
Kyoto University Research Information Repository
https://repository.kulib.kyoto-u.ac.jp
京都大学学術情報リポジトリ KURENAI 紅 Kyoto University Research Information Repository

B. *Frequency response measurement*

Fig.6 is the measurement set-up of both the frequency response and angular rate detection experiments. The ring resonator was connected to the ground and the red and blue colored electrodes were biased to 5 V (not drawn) for mainly displacement detection, but also for symmetry of electrostatic force. For driving, ac sinusoidal voltage was added to the bottom blue electrode for 0°-drive and the top-right red electrode for 45°-drive. The top blue and bottom-left red electrodes were connected charge amplifier for 0°- and 45°-displacement detections, respectively. For electrostatic tuning on the angular rate detection, we used the four electrodes, $T_{+22.5}$, T_0, $T_{-22.5}$ and T_{-45} on the right-bottom of the resonator. The circuit and packaged device were put in a custom-made vacuum chamber with a rotation table. The frequency response of each mode was measured by applying ac voltage of 10 mV amplitude using a digital lock-in amplifier (MF-LI, Zurich Instruments).

C. *Gyro operation*

The angular rate detection was conducted using the same set-up described in the previous section. The driving and sensing controls were made using a digital lock-in amplifier (HF2LI, Zurich Instruments) [6]. For driving (0° mode), closed loop operation using the phase locked loop (PLL) and automatic gain control (AGC). For sensing, the open-loop rate detection operation was used where the sense mode (45° mode) displacement output is demodulated by the reference signal from the PLL for driving. Constant angular rates up to ±120° were applied and the demodulated output voltage difference were measured.

IV. Results and Discuss

A. *Frequency response*

Fig. 7 shows a fabricated device. The frequency response of 13 resonators were measured, as shown in Fig. 8. The

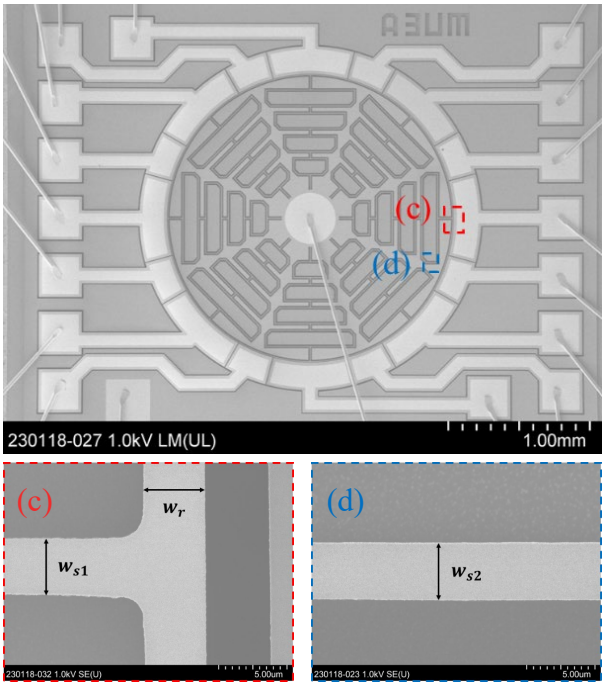

Fig. 7. Fabricated ring resonator. (c) and (d) show close-up viewes at ring suspended part and rectanglar spring part, respectively.

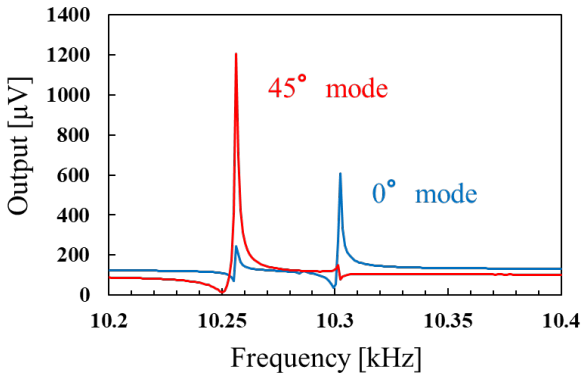

Fig. 8. Typical frequency response of ring resonator without any electrical tunings.

resonant frequencies and the mode mismatch ranged from 9.95 to 12.18 kHz and from 46 to 144 Hz, respectively. Although there were large deviations in width indicated by the measured resonant frequencies, the deviations of the mode mismatch is relatively small compered to the previous research owing to our spring design. However, the mode mismatch is larger than expected. To investigate the reason, we measured the widths of the beams of the ring and suspensions at the position indicated in Fig. 7. The difference in the beam width in the suspension W_{s1} and W_{s2} is ranged from 10 to 60 nm, which is small. However, the width difference between the suspension beam and ring beam were large, ranged from 300 to 550 nm, though it was designed as 100 nm ($W_{s1} = W_{s2} = 5.0$ μm and $W_r = 5.1$ μm). The reason of large difference of dimensional errors were caused by the loading effect in silicon deep RIE, where the ring has the narrow gap (3 or 4 μm) for electrostatic actuation and sensing. We thought that the smaller gap shows the smaller dimensional errors in fabrication. In addition, the measured frequencies were much smaller than the simulation owing to narrowing of the width. The fabrication process should be improved.

B. *Angular rate output*

For angular rate detection, the remaining mode mismatch is compensated using the electrostatic force at the tuning electrodes. The smallest mode-mismatch resonator of 46 Hz was used and mode matching is realized at $T_{-45} = T_{-22.5} = 0$ V, $T_0 = 5.8$ V and $T_{+22.5} = 5.58$ V. The scale factor plot is shown in Fig. 9. The scale factor is 3.8 μV/°/sec, which is much larger than our previous report [7], where the same measurement setups were used. The bias stability was 278°/h and the angle

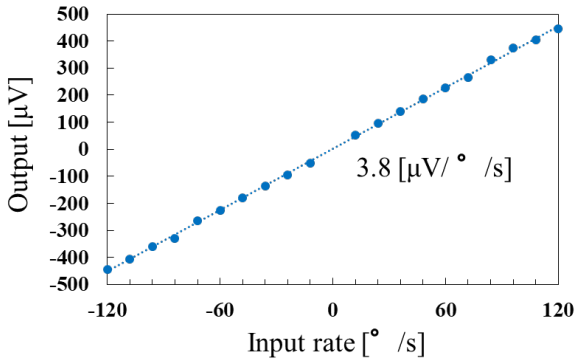

Fig. 9. Scale factor plot of mode-matched ring vibrating gyroscope.

京都大学 KYOTO UNIVERSITY
A Self-archived copy in
Kyoto University Research Information Repository
https://repository.kulib.kyoto-u.ac.jp
京都大学学術情報リポジトリ KURENAI 紅 Kyoto University Research Information Repository

random walk was 25°/$\sqrt{\text{Hz}}$. Due to single detection at the displace measurement, the circuit noise became large. By using differential detection using orthogonal electrodes, both the bias stability and ARW will be improved.

V. Conclusion

A new suspension spring structure with series of chamfered rectangular beams was proposed for the ring resonator using (100) single crystal silicon for mode-matched vibratory gyroscope. Although the simulation assuming uniform dimensional errors during fabrication showed good robustness against the errors for keeping mode matching, the fabricated results were worse because of the nonuniform dimensional errors caused by the loading effect in silicon etching. We are now trying to reduce the dimensional errors and their nonuniformity by modifying the photomask design and process conditions to demonstrate the potential of the proposed design.

Acknowledgment

This work is supported by JSPS KAKENHI Grant Numbers JP22K18289 and Kyoto University Nanotechnology Hub in the “ARIM Project” sponsored by MEXT, Japan.

References

[1] Y. Shu, Y. Hirai, T. Tsuchiya, and O. Tabata, “Geometrical Compensation for Mode-Matching of (100) Silicon Ring Resonator for Vibratory Gyroscope,” Jpn. J. of Appl. Phys. vol. 58, art. No. SDDL06 (2019)

[2] C. H. Ahn, E. J. Ng, V. A. Hong, Y. Yang, B. J. Lee, I. Flader, T. W. Kenny, “Mode-Matching of Wineglass Mode Disk Resonator Gyroscope in (100) Single Crystal Silicon,” Journal of Microelectromechanical Systems, vol. 24, pp. 343-350, April 2014.

[3] S. Nitzan, C. H. Ahn, T.-H. Su, M. Li, E. J. Ng, S. Wang, Z. M. Yang, G. O'Brien, B. E. Boser, T. W. Kenny, D. A. Horsley, “Epitaxially-encapsulated polysilicon disk resonator gyroscope,” Proc. IEEE MEMS 2013, pp. 625-628

[4] J. Cho, J.A. Gregory, and K. Najafi, “Single-crystal-silicon vibratory cylinderical rate integrating gyroscope (CING),” J. Cho, J.A. Gregory, K. Najafi, Proc. Transducers 2011, pp. 2813-2816

[5] T. Tsukamoto and S. Tanaka, “Fully-differential single resonator FM/whole angle gyroscope using CW/CCW mode separator,” Proc. IEEE MEMS 2017, pp. 1118-1121

[6] Zurich Instruments. Application Note: Control of MEMS Coriolis Vibratory Gyroscopes. Accessed: Feb. 6, 2023. [Online]. Available: https://www.zhinst.com/sites/default/files/zi_appnote_mems_gyroscope.pdf

[7] Y. Shu, Y. Hirai, T. Tsuchiya, “Scale-Factor Analysis of a Geometrically Compensated (100) Single-Crystal Silicon Vibratory Ring Gyroscope, The 7th IEEE International Symposium on Inertial Sensors and Systems (INERTIAL 2020), Hiroshima, Japan, (March 23-26, 2020).